How Important Is the Dispersion Interaction for Cyclobis(paraquat-*p*-phenylene)-Based Molecular "Shuttles"? A Theoretical Study

CARLOS ROMERO, LIOUDMILA FOMINA, SERGUEI FOMINE

Instituto de Investigaciones en Materiales, Universidad Nacional Autónoma de México, Apartado Postal 70-360, CU, Coyoacán , México DF 04510, México

Received 27 June 2004; accepted 4 August 2004
Published online 17 November 2004 in Wiley InterScience (www.interscience.wiley.com).
DOI 10.1002/qua.20360

ABSTRACT: Inclusion complexes of cyclobis(paraquat-*p*-phenylene) and various aromatic molecules in their neutral and oxidized form were studied at the LMP2/6-311+G**//BHandHLYP/6-31G* level of theory, which represents the highest level theoretical study to date for these complexes. The results show that it is dispersion interaction that contributes most to the binding energy. One electron oxidation of a guest molecule leads to complete dissociation of inclusion complex generating strong repulsion potential between guest and host molecules. Electrostatic interactions also can play an important role, provided the guest molecule has a dipole moment; however, dispersion interactions always dominate in binding energy. Int J Quantum Chem 102: 200–208, 2005

Key words: ab initio calculations; computer chemistry; density functional calculations; host guest systems; noncovalent interactions

Introduction

Artificial molecular machines appear as one of the emerging fields of chemistry in the past decade [1]. Several such systems have been designed recently, many of them being based on electroactive compounds whose shape will be modified at will by a redox process. One representative example of "molecular machines," depicted in Figure 1, is based on organic acceptor–donor interactions in a rotoxane. A rotaxane [2] is a molecular system consisting of a ring threaded by a string with two blocking groups attached. Such compounds were made long ago [2, 3], but they have been mostly considered chemical curiosities. Recently, rotaxanes underwent a real revival because of their electro- and photochemical properties [4–6] and their ability to undergo controlled molecu-

Correspondence to: S. Fomine; e-mail: fomine@servidor.unam.mx

Contract grant sponsor: Dirección general de apoyo academico (DGAPA).

Contract grant number: IX-102404/14.

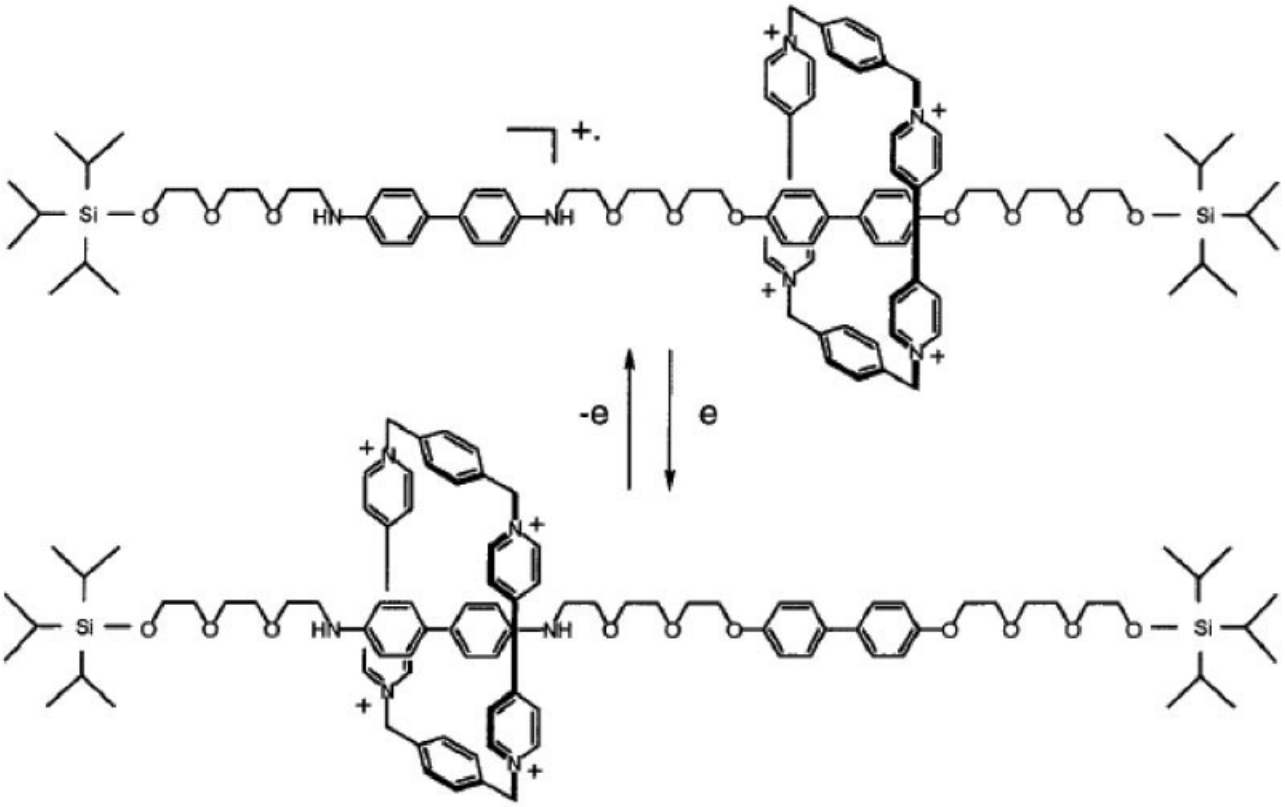

FIGURE 1. An example of molecular "shuttle" based on cyclobis(paraquat-*p*-phenylene) synthesized in [7].

lar motions [7–9]. The molecular machine depicted in Figure 1 represents a molecular "shuttle," where molecular movement is induced by one electron oxidation-reduction of the donor part of rotoxane (benzidine fragment). The controlled molecular movement in this system is dependent to a great extent on the differences in complexation energies between the neutral and oxidized form of a donor fragment. The larger the difference the better control of the molecular movement can be achieved by switching between two states. Therefore, the understanding and quantification of interactions between moving parts of a molecular machine is essential for their rational design.

A few theoretical studies have been published of host–guest complexes at the molecular mechanics [10, 11] or semiempirical levels [12–14]. In a limited number of studies paraquat-containing complexes were treated at the Hartree-Fock or DFT (Density Functional Theory) levels [12–18]. However, in many cases these methods are not adequate to correctly describe intermolecular interactions. Even Hartree-Fock and many of the DFT methods, including the popular hybrid B3LYP functional, produce qualitatively wrong results due to a missed correlation energy term when treating weakly bounded complexes [19]. One recent and the most high-level study of paraquat–organic donor complexes uses B3LYP functional for geometry optimization and the MP2 method for energy evaluation. The most intriguing guess of this study is that the stability of these complexes is primarily due to dispersion interactions [20]. Since the B3LYP functional is not adequate to describe dispersive interactions [19], it is necessary to consider a more adequate method for geometry optimization of paraquat-containing complexes.

This article represents the first attempt to estimate quantitatively interactions which are responsible for the functioning of the molecular "shuttle" shown in Figure 1 using more adequate methods for both geometry optimization and energy evaluation and to create a theoretical basis for directional design of molecular "shuttles" based on redox reactions.

Computational Details

Figure 2 shows the model system used for this study. A large number of atoms to be treated at the

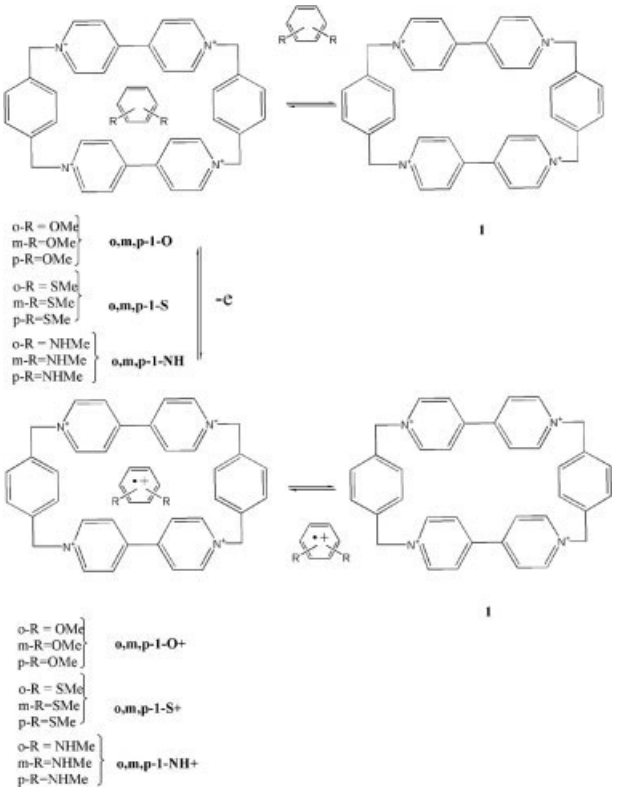

FIGURE 2. Model systems used for calculations.

post-Hartree-Fock theoretical level forces one to adopt a model of reasonable size, yet maintaining all important features of the original system. Since two factors are of mayor importance for host–guest chemistry, the electronic and steric complexes with *o*-, *p*-, and *m*-disubstituted benzenes bearing methoxy, methylamino, and methylsulphide groups were studied. To obtain quantitative information about interactions in the model system a method taking into account electron correlation should be used. A popular MP2 method widely used for the study of intermolecular interactions [21–24] is prohibitive for geometry optimization due to the size of the problem. DFT methods are much less computationally demanding, although it has been shown that they often fail in the case where dispersion stabilization represents the main contribution to the binding energy [19]. It has been shown, however, that a half-and-half functional is successful in the prediction of energetic and geometry for halogen–ethylene van der Waals complexes giving results very close to that of the MP2 method [25] and a DFT method using empirical dispersion energy was successfully used to describe intermolecular complexes [26]. Therefore, a complex approach to the modeling of host–guest complexes was applied: DFT geometry optimization and MP2 single point energy evaluation. Figure 3 shows the optimized geometry of a model complex between 1,4-dimethoxybenzene and *N*-methyl pyridinium cation optimized at MP2/6-31G* and BHandHLYP/6-31G* method. This model system has the same type of groups as paraquat inclusion complexes and represents a reasonable model to test the performance of different methods. As seen, these geometries are very similar. On the other hand, the tested B3LYP/6-31G* and B3PW91/6-31G* models produced geometries for 1,4-dimethoxybenzene – *N*-methyl pyridinium cation complexes which are qualitatively different from that obtained with the MP2 method. All geometry optimizations were carried out at the BHandHLYP/6-31G* level in gas phase without any geometry restrictions.

To estimate binding energies of the studied complexes the local implementation of the MP2 method (LMP2) was used as implemented in the jaguar 5.0 suite of programs [27] in combination with a large 6-311+G** basis set. The local MP2 approach was shown to have some advantages compared to the canonical MP2 method in studying intermolecular complexes [28]; moreover, the LMP2 method gives reliable results in describing hydrogen bonds at substantially lower computational cost than canonical MP2 [29, 30]. A detailed description of the LMP2 approach is given in Ref. 30. All DFT and MP2 geometry optimizations were carried out using jaguar 5.0 and Gaussian 03 [31] suites of programs, respectively. Unrestricted formalism was used to treat open shell systems at the DFT level, while for LMP2 calculations, the restricted open shell method was applied. All binding energies were corrected for basis set superposition error according to Ref. 32. The orientation of guest molecules in complexes was selected based on available X-ray data [33].

Results and Discussion

Table I and Figure 4 show selected measurements and general views of optimized geometries of cycle **1** and corresponding complexes. Apparently, the geometry of inclusion complexes is not affected seriously by the optimization method. Thus, complex **p-1-O** has been studied previously with the B3LYP/6-31G** method [20]. The complex geometry was qualitatively similar to that obtained

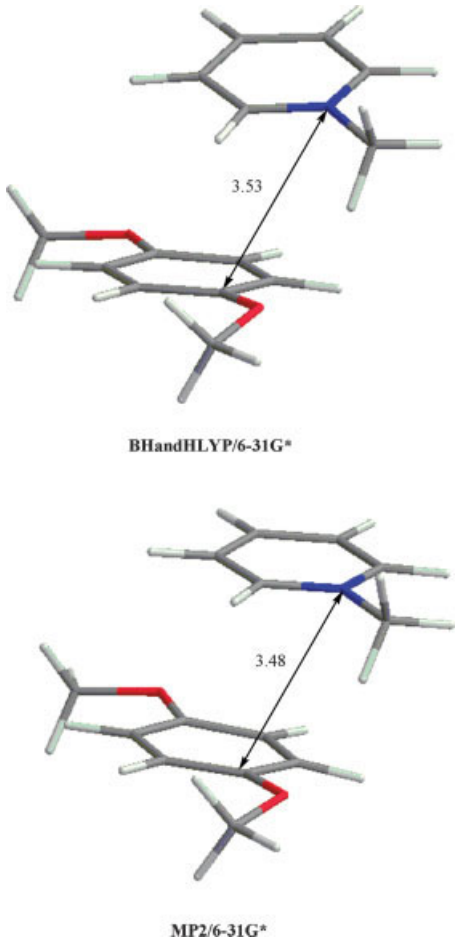

FIGURE 3. Geometries of intermolecular complex between ion de *N*-methylpyridinium and 1,4-dimethoxybenzene optimized at different levels of theory.

in this study using BHandHLYP functional. When comparing B3LYP/6-31G** [20] with BHandHLYP/6-31G* structures of **p-1-O**, $\mathbf{R_1}$ is 0.27 and $\mathbf{R_2}$ is 0.1 Å longer. The qualitative agreement between these methods is due to the fact that guest molecule movements are very much restricted inside the cavity and the complex geometry is primarily defined by steric factors. On the other hand, when binding energies are compared there is a striking difference between the methods. Thus, the B3LYP/6-31G** model predicts the binding energy for complex **p-1-O** to be of −4.9 kcal/mol [20], while the BHandHLYP/6-31G* model gives –17.2 kcal/mol. On the other hand, the MP2/6-31G**//B3LYP/6-31G** model [20] predicts the binding energy for this complex to be of –24.2 kcal/mol, which is very different from the B3LYP/6-31G** model and agrees much better with the prediction of the BHandHLYP/6-31G* method. The highest level to date binding energy evaluation carried out for this complex (LMP2/6-311+G** level) using BHandHLYP/6-31G* geometry predicts the **p-1-O** complex to have a binding energy of –21.3 kcal/mol (Table II), which is in reasonable agreement with MP2/6-31G** and BHandHLYP/6-31G* energies and very different from the B3LYP/6-31G** model. Thus, extreme care should be taken when using B3LYP functional for the study of a system when dispersion interaction is important.

When analyzing the connection between the geometries of cycle **1** in complexes and the shape of the guest molecule (Table I), one can observe that the $\mathbf{R_2}$ distance in complexes vary by 0.26 Å and $\mathbf{R_1}$ changes by 0.54 Å, which is definitely related to the much stronger face-to-face interactions compared to face-to-edge ones [20]. Within each group of guest molecules the smallest $\mathbf{R_1}$ is for derivatives of phenylenediamines, while the largest is for derivatives of dithiolbenzenes. As seen from Tables I and II, there is clear correlation between $\mathbf{R_1}$ and binding

TABLE I

Selected geometrical parameters of minimized host–guest complexes and a free cycle.

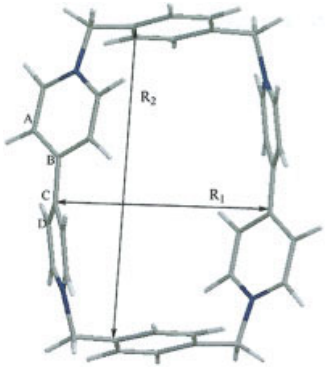

Complex	Dihedral ABCD (°)	$\mathbf{R_1}$(A)	$\mathbf{R_2}$(A)
o-1-O	39.3	7.75	9.82
m-1-O	22.5	7.57	9.91
p-1-O	36.4	7.53	9.92
o-1-NH	36.1	7.60	9.85
m-1-NH	31.9	7.37	10.0
p-1-NH	31.6	7.49	9.92
o-1-S	35.9	7.80	9.81
m-1-S	31.9	7.82	9.74
p-1-S	38.0	7.68	9.91
p-1-NH+	27.9	7.91	9.73
1	36.2	7.61	9.88

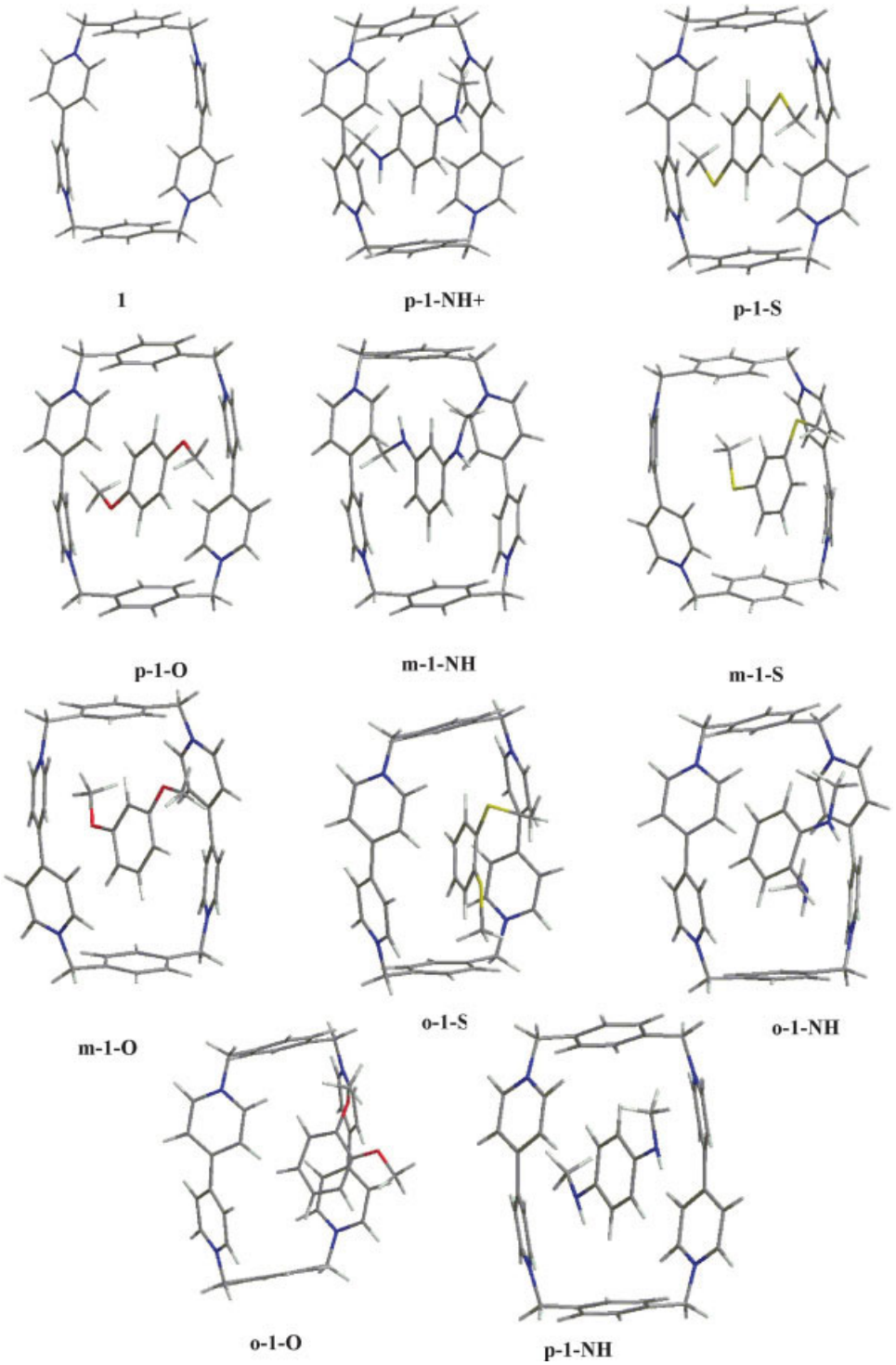

FIGURE 4. BHandHLYP/6-31G* optimized geometries of cyclobis(paraquat-*p*-phenylene) inclusion complexes.

energy (at LMP2 and BHandHLYP levels) for O- and *N*-substituted guests. The smaller the distance, the higher is the binding energy. In the case of S-substituted guests, $\mathbf{R_1}$ is larger due to bulky substituents. When comparing o-, *m*-, and *p*-disubstituted guests it is seen that o-substituted guest mol-

TABLE II

Total energies of host cycle (E_3), donor guest molecules (E_2) (a.u.), BSSE-corrected binding energies of host–guest complexes (E_4) and cycle 1 deformation energies (E_5) (kcal/mol) at different levels of theory.

complex	E_1	E_2	E_3	E_4	E_5[a]
			BHandHLYP/6-31G*		
o-1-O	−2048.86230	−457.72604	−1592.093438	−22.1	0.4
m-1-O	−2048.86153	−456.73758		−13.1	1.0
p-1-O	−2048.86419	−456.73036		−17.2	0.8
o-1-NH	−2009.27494	−417.14576		−19.8	1.8
m-1-NH	−2009.282036	−417.14716		−19.6	0.7
p-1-NH	−2009.27684	−417.14199		−19.6	0.7
o-1-S	−2693.32692	−1101.20242		−15.9	0.6
m-1-S	−2693.341177	−1101.20362		−23.1	0.6
p-1-S	−2693.34096	−1101.20292		−22.7	0.6
p-1-NH+	−2008.72724	−416.94777		200.7	1.1
			LMP2/6-311+G**//BHandHLYP/6-31G*		
o-1-O	−2064.238988	−460.041742	−1604.159036	−21.0(−12.2)[b]	0.0
m-1-O	−2064.236958	−460.052055		−16.1(−22.1)	1.7
p-1-O	−2064.244532	−460.047542		−21.3(−21.6)	1.4
o-1-NH	−2024.556233	−420.365993		−22.3(−25.1)	1.9
m-1-NH	−2024.559164	−420.362977		−22.5(−24.6)	2.4
p-1-NH	−2024.562521	−420.333766		−23.9(−23.7)	1.5
o-1-S	−2709.441117	−1105.253035		−18.2(20.4)	0.5
m-1-S	−2709.454238	−1105.255737		−22.7(−20.8)	0.6
p-1-S	−2709.459299	−1105.255538		−25.3(−23.7)	0.3
p-1-NH+	−2023.985451	−420.123041		186.0(−27.9)	0.0
			HF/6-311+G**//BHandHLYP/6-31G*		
o-1-O	−2057.367947	−458.566219	−1598.781861	−8.8	0.7
m-1-O	−2057.353992	−458.579248		6.0	1.4
p-1-O	−2057.359390	−458.573671		0.3	1.0
o-1-NH	−2017.689487	−418.915284		2.8	1.7
m-1-NH	−2017.698876	−418.918998		2.1	2.0
p-1-NH	−2017.697099	−418.867933		−0.2	1.1
o-1-S	−2702.675884	−1103.897733		2.2	0.5
m-1-S	−2702.688848	−1103.899841		−1.9	0.7
p-1-S	−2702.689046	−1103.901470		−1.6	0.3
p-1-NH+	−2017.152692	−418.710031		213.9	1.4

[a] Defined as the difference between the total energy of cycle 1 in complex and that of free cycle 1.
[b] Correlation stabilization energy, defined as E_4(LMP2)-E_4(HF).

ecules do not form truly inclusion complexes due to an inappropriate shape. This is reflected in generally larger $\mathbf{R_1}$ compared to other isomers. The smaller $\mathbf{R_1}$ for *p* and *m*-isomers is due to a more favorable shape.

The driving force making the molecular "shuttle" shown in Figure 1 work is the oxidation of a donor molecule, causing dissociation of the molecular complex. The geometry optimization of ionized complexes starting from the geometry of initial inclusion complexes causes dissociation of all inclusion complexes but **p-1-NH+** (Fig. 2). This oxidized species is has extremely positive binding energy (Table II) and the largest $\mathbf{R_1}$ distance of 7.91 Å, reflecting strong electrostatic repulsion between positive guest and host molecules. Thus, the oxidation of the **p-1-NH** molecule increases $\mathbf{R_1}$ from 7.49 to 7.91 Å, while $\mathbf{R_2}$ decreases from 9.92 to 9.73 Å. It

is noteworthy that the overall structure of the complex is not changed upon oxidation (Fig. 4).

It is interesting to analyze the deformation energy of a cycle in a complex which corresponds to the energy difference between a cycle with conformation in a complex and a free cycle. As can be noted from Table II, this energy is within 2 kcal/mol in almost all cases, which is within the precision provided by applied computational methods and, therefore, can be discarded. This is not the case for dispersion interactions. When analyzing the binding energies of inclusion complexes at the HF and MP2 level, one can estimate the contribution of correlation energy to the complex stabilization by the difference of binding energy at different levels of theory. As seen (Table II), the stabilization energy of inclusion complexes is almost completely due to correlation stabilization, while the stabilization at HF the level (electrostatic, polarization, repulsive exchange, and charge transfer) represents only a small portion of total stabilization energy. In the case of **p-1-NH+** oxidized complex the interaction between host and guest consists of strong electrostatic repulsion; however, as seen from the Table II, dispersion stabilization reduces the repulsive interaction at the HF level by 28 kcal/mol.

Since LMP2 does not generate BSSE at the MP2 level [34] and HF energy is saturated relatively fast with a basis set size LMP2/6-311+G** CP-corrected binding energies must be very close to genuine binding energies. Thus, it has been shown [35] that for various aromatic dimers LMP2/aug-cc-pVTZ(-f) binding energies do not need CP correction. When comparing LMP2 and BHandHLYP stabilization energies of inclusion complexes, one can observe that there is very good correlation between the two methods, showing that BHandHLYP functional correctly describes interaction in the inclusion complexes of **1**.

Available experimental data on the formation of inclusion complexes by molecule **1** show that nitrogen-substituted aromatic molecules bind to **1** with greater affinity than oxygen-substituted systems and 4,4′-substituted biphenyl molecules bind to **1** better than 1,4-substituted phenyl derivatives [16]. The greater affinity of biphenyl compared to benzene derivatives supports the conclusion about the importance of dispersion energy for complex stabilization. Both LMP2 and BHandHLYP results predict nitrogen-substituted aromatic molecules bind to **1** with greater affinity compared to oxygen ones, except for **o-1-NH** and **o-1-O**.

TABLE III

Dipole moment (D), ionization potential (IP) (eV) and average polarizabilities (a.u.) of guest molecules calculated at BHandHLYP/6-31G* level.

Guest molecule	Dipole moment	IP[a] (eV)	Average polarizability[b]	NPA Charge[c]
o-$(MeO)_2$Ph	2.3	6.61	85.4	0.026
m-$(MeO)_2$Ph	1.3	6.88	85.6	0.006
p-$(MeO)_2$Ph	1.8	6.43	85.3	0.008
o-$(MeNH)_2$Ph	1.2	5.92	93.6	0.019
m-$(MeNH)_2$Ph	1.3	5.72	95.2	0.022
p-$(MeNH)_2$Ph	2.1	5.29	98.0	0.017
o-$(MeS)_2$Ph	2.9	6.71	113.6	0.019
m-$(MeS)_2$Ph	1.5	6.83	115.3	0.0026
p-$(MeS)_2$Ph	2.2	6.47	116.5	0.017

[a] Adiabatic ionization potential calculated as E^+-E, where E^+ is the energy of cation-radical at equilibrium geometry and E is that of neutral molecule.
[b] Defined as 1/3 ($\alpha_{xx} + \alpha_{yy} + \alpha_{zz}$).
[c] Natural charge of donor molecule in complex calculated at MP2/6-31G* level.

To gain deeper insight into the nature of interactions between donor molecules and host **1**, various physical properties of the donor molecules were calculated (Table III). As seen, there is no correlation between ionization potential (IP) and binding energies of complexes discarding significant electron transfer from donor molecules. Natural charges calculated at the MP2/6-31G* level for donor part of complexes listed in Table III show that electron transfer is minimal and there is no correlation between IP of donor and their natural charge. On the other hand, molecular polarizabilities calculated for donor molecules correlate with binding energies of complexes. Thus, according to Table III molecular polarizabilities increase in the order: oxygen, nitrogen, sulfur derivatives, which is in line with an increase of binding energies in the same direction. The only exception for this trend is observed for o-isomers.

When comparing correlation stabilization energies of complexes with molecular polarizabilities of donor molecules, one can observe that the most negative correlation stabilization is for nitrogen-containing guests and not for sulfur-containing ones having larger polarizabilities. This phenomenon is due to the larger size of *S*-containing donors and a larger donor–acceptor distance, as follows from Table I. The dispersion contribution in binding energy can be written as a sum of three terms [36]:

$$\Delta E_{\text{disp}} = -[C_6/r^6 + C_8/r^8 + C_{10}/r^{10}] \qquad (1)$$

where dipole–dipole (r^{-6}), dipole quadrupole (r^{-8}), and quadrupole–quadrulole (r^{-10}) terms are taken into account and C_n are dispersion coefficients. As can be seen from Eq. (1), ΔE_{disp} decreases strongly with intermolecular distance, and at the distances where the overlap of valence shells can be neglected the correlation energy has a physical meaning of dispersion energy [36]. Therefore, there is a decrease of dispersion and as a consequence correlation stabilization of complexes of *S*-containing complexes can be related to bulky sulfur atoms. This explanation is supported by the relatively low correlation stabilization for o-isomers bearing oxygen and sulfur side groups. The correlation stabilization in LMP2 formalism can be represented as a sum of inter- and intramolecular correlation contributions [37]. The dispersion energy is a part of intermolecular correlation and represents an attractive part of intermolecular stabilization energy, while the numerical results on NH_3-H_2O complexes [37] show that intramolecular correlation energy is repulsive and the relative importance of the intramolecular correlation term decreases with intermolecular distance. Thus, the increase in stability of paraquat complexes at the LMP2 level compared to HF is related to dispersion stabilization.

Complexes **o-1-O** and **o-1-S** are rather loose due to an unfavorable molecular shape. On the other hand, **o-1-NH** forms a tight complex similar to those formed by *m* and *p* isomers. The difference between them can be understood by inspecting the geometry of the **o-1-NH** complex, where NH-π bonding exists which follows from a slightly larger NH bond (1.02 Å) compared to 1.01 Å in **p-1-NH** and relatively short (2.51 Å) H-aromatic plane distance.

Experimental observation that electron-withdrawing groups reduce binding [16] can be rationalized in terms of polarizability instead of electrostatic interaction due to partial electron transfer. Electron-donating side groups as a rule increase polarizability of a molecule, while electron-withdrawing groups decrease it. On the other hand, Table III shows that although *m*- and *p*-N,N′-dimethyl phenylenediamines are stronger donors than corresponding S-containing guests, the binding energies at the LMP2 level are higher for the latter, which is in line with polarizabilities of these molecules.

In the case of perceptible dipole moment of guest molecules, electrostatic interactions can also make a remarkable contribution in total binding energy. When analyzing HF binding energies of supramolecular complexes, one can see a rather negative value of −8.8 kcal/mol (Table II) for **o-1-O**, which can be attributed to a relatively large dipole moment (2.3 D) of guest molecule. In a recent article [38], it was shown that C-H…O interaction in methylpyridinium–dimithyl ether complex are electrostatic by nature, which could be responsible for this result. Another indirect confirmation of relative importance of electrostatic interactions is experimental data [16] showing that the binding constant for p-aminophenol is larger than for p-phenylenediamine. It is difficult, however, to observe a direct correlation between HF binding energies of complexes and dipole moments of guest molecules due to the complex nature of HF binding energy. Apart from electrostatic interactions, HF energy includes exchange repulsion, polarization, charge transfer, and other terms.

Conclusions

Calculations show unambiguously that the origin of stability of cyclobis(paraquat-*p*-phenylene) inclusion complexes with donor molecules is a dispersion interaction which can contribute up to 100% to the binding. This finding is in agreement with all available experimental data. The binding energies calculated here are based on the highest level calculation performed to date for these types of systems and they are believed to be very close to genuine binding energies. Since dispersion interactions are very distance-sensitive, the shape of a guest molecule plays an important role. Although dispersion stabilization represents the main contribution to the stabilization energy, guest molecules having dipole moment impart additional stability to the complex due to electrostatic interaction. The oxidation of a guest molecule not only decreases stability of the supramolecular complex, but creates an extremely powerful repulsive potential (around 200 kcal/mol) between guest and host molecules, leading to its complete dissociation. Since the oxidation of a guest molecule creates such a strong repulsion between guest and host molecules, therefore low oxidation potential and high polarizability of a guest molecule are the keys features to take into account when designing a molecular "shuttle" based on cyclobis(paraquat-*p*-phenylene) host.

References

1. (a) Balzani, V.; Gómez-López, M.; Stoddart, J. F. Acc Chem Res 1998, 31, 405; (b) Sauvage, J.-P. Acc Chem Res 1998, 31, 611; (c) Fabbrizzi, L.; Licchelli, M.; Pallavicini, P. Acc Chem Res 1999, 32, 846; (d) Kelly, T. R.; De Silva, H.; Silva, R. A. Nature 1999, 401, 150; (e) Koumura, N.; Zijlstra, W. J.; Van Delden, R. A.; Harada, N.; Feringa, B. L. Nature 1999, 401, 152; (f) Balzani, V.; Credi, A.; Raymo, F. M.; Stoddart, J. F. Angew Chem Int Ed 2000, 39, 3348.
2. Schill, G.; Zollenkopf, H.; Rotaxan-Verbindungen, I. Liebigs Ann Chem 1969, 721, 53.
3. Harisson, I. T.; Harrison, S. J Am Chem Soc 1967, 89, 5723.
4. Chambron, J.-C.; Harriman, A.; Heitz, V.; Sauvage, J.-P. J Am Chem Soc 1993, 115, 6109.
5. Diederich, F.; Dietrich-Buchecker, C.; Nierengarten, J.-F.; Sauvage J.-P. J Chem Soc Chem Commun 1995, 781.
6. Zhu S. S.; Carroll, P. J.; Swager, T. M. J Am Chem Soc 1996, 118, 8713.
7. Bissell, R. A.; Córdova, E.; . Kaifer, A.E.; Stoddart, J.F. Nature 1994, 369, 133.
8. Ballardini, R.; Balzani, V.; Gandolfi, M. T.; Prodi, L.; Venturi, M.; Philp, D.; Ricketts, H. G.; Stoddart, J. F. Angew Chem Int Ed Engl 1993, 32, 1301.
9. Gaviña, P.; Sauvage, J.-P. New J Chem 1997, 21, 525.
10. Approaches in Supramolecular Chemistry; Wipff, G. Ed.; Kluwer Academic: Boston, MA, 1994.
11. Kaminski, G. A.; Jorgensen, W. L. J Chem Soc Perkin Trans 2 1999, 2365.
12. Castro, R.; Davidov, P. D.; Kumar, K. A.; Marchand, A. P.; Evanseck, J. D.; Kaifer, A. E. J Phys Org Chem 1997, 10, 369.
13. Zhang, K.-C.; Liu, L.; Mu, T.-W.; Guo, Q.-X. J Inclusion Phenom 2001, 40, 189.
14. Zhang, K.-C.; Liu, L.; Mu, T.-W.; Guo, Q.-X. Chem Phys Lett 2001, 333, 195.
15. D'Acerno, C.; Doddi, G.; Ercolani, G.; Mencarelli, P. Chem Eur J 2000, 6, 3540.
16. Castro, R.; Berardi, M. J.; Córdova, E.; Ochoa de Olza, M.; Kaifer, A. E.; Evanseck, J. D. J Am Chem Soc 1996, 118, 10257.
17. Zhang, K-C.; Liu, L.; Mu, T-W.; Guo, Q-X. Chem Phys Lett 2001, 333, 195.
18. Castro, R.; Davidov, P. D.; Kumar, K. A.; Marchand, A. P.; Evanseck, J. D.; Kaifer, A. E. J Phys Org Chem, 1997, 10, 369.
19. Chałasinski, G.; Szczeüsniak, M. M. Chem Rev 2000, 100, 4227.
20. Ercolani G.; Mencarelli, P. J Org Chem 2003, 68, 6470.
21. Kim, K. S.; Tarakeshwar, P.; Lee, J. Y. Chem Rev 2000, 100, 4145.
22. Tsuzuki, S.; Honda, K.; Uchimaru, T.; Mikami, M.; Tanabe, K. J Am Chem Soc 2002, 124, 104.
23. Sponer, J.; Leszczynski, J.; Hobza, P. J Comp Chem 1996, 17, 841.
24. Hobza, P.; Kabelac, M.; Sponer, J.; Mejzlik, P.; Vondrasek, J. J Comp Chem 1997, 18, 1136.
25. Ruiz, E.; Salahub D. R.; Vela, A. J Am Chem Soc 1995, 117, 1141.
26. Reha, D.; Kabelac, M.; Ryjacek, F.; Sponer, J.; Sponer, J. E.; Elstner, M.; Suhai, S.; Hobza, P. J Am Chem Soc 2002, 124, 3366.
27. Jaguar 5.0, Schrodinger, LLC, Portland, Oregon, 2003.
28. Reyes, A.; Tlenkopatchev, M. A.; Fomina, L.; Guadarrama, P.; Fomine, S. J Phys Chem A, 2003 107, 7027.
29. Huang, N.; MacKerell, A. D. Jr. J Phys Chem A 2002, 106, 7820.
30. Schu1tz, M.; Rauhut, G.; Werner H-J. J Phys Chem A 1998, 102, 5997.
31. Gaussian 03, Revision B.04, Frisch, M. J.; Trucks, G. W.; Schlegel, H. B.; Scuseria, G. E.; Robb, M. A.; Cheeseman, J. R.; Zakrzewski, V. G.; Montgomery, J. A.; Stratmann, R. E.; Burant, J. C.; Dapprich, S.; Millam, J. M.; Daniels, A. D.; Kudin, K. N.; Strain, M. C.; Farkas, O.; Tomasi, J.; Barone, V.; Cossi, M.; Cammi, R.; Mennucci, B.; Pomelli, C.; Adamo, C.; Clifford, S.; Ochterski, J.; Petersson, G. A.; Ayala, P. Y.; Cui, Q.; Morokuma, K.; Salvador, P.; Dannenberg, J. J.; Malick, D. K.; Rabuck, A. D.; Raghavachari, K.; Foresman, J. B.; Cioslowski, J.; Ortiz, J. V.; Baboul, A. G.; Stefanov, B. B.; Liu, G.; Liashenko, A.; Piskorz, P.; Komaromi, I.; Gomperts, R.; Martin, R. L.; Fox, D. J.; Keith, T.; Al-Laham, M.; Peng, C.; Nanayakkara, A.; Challacombe, M.; Gill, P. M. W.; Johnson, B. G.; Chen, W. Wong, M. W.; Andres, J. L.; Gonzalez, R.; Head-Gordon, M.; Replogle, E. S.; Pople, J. A. Gaussian, Pittsburgh, PA, 2003.
32. Boys, S. F.; Bernardi, F. Mol Phys 1970, 19, 553-566.
33. Anelli, P. L.; Ashton, P. R.; Ballardini, R.; Balzani, V.; Delgado, M.; Gandolfi, T. T. Goodnow, M.-T.; Kaifer, A. E.; Philp, D.; Pietraszkiewicz, M.; Prodi, L.; Reddington, M. V.; Slawin, A. M. Z.; Spencer, N.; Stoddart, J. F.; Vicent, C.; Williams, D. J. J Am Chem Soc 1992 114, 193.
34. Saebo, S.; Pulay, P. J Chem Phys 1993, 98, 2170.
35. Fomine, S.; Tlenkopatchev, M.; Martinez, S.; Fomina, L. J Phys Chem 2002 106, 3941.
36. Kaplan, I. G.; Rozak, S.; Leszczynsky, J. J Chem Phys 2000, 113, 6245.
37. Langlet, J.; Caillet, J.; Berges, J.; Reinhardt, P. J Chem Phys 2003, 118, 6157.
38. Raymo, F. M.; Bartberger, M. D.; Houk, K. N.; Stoddart J. F. J Am Chem Soc 2001, 123, 9264.